

An Automated Algorithm for Online Detection of Fragmented QRS and Identification of its Various Morphologies

Sidharth Maheshwari¹; Amit Acharyya^{2,*}; Paolo Emilio Puddu³; Evangelos B. Mazomenos⁴; Gourav Leekha⁵; Koushik Maharatna⁴; Michele Schiariti³

¹Electronics and Electrical Engineering, Indian Institute of Technology Guwahati, Guwahati, India

²Department of Electrical Engineering, Indian Institute of Technology Hyderabad, Hyderabad, India

³Department of Cardiovascular Sciences, Sapienza University of Rome, Rome, Italy

⁴School of Electronics and Computer Science, University of Southampton, SO17 1BJ, UK

⁵Department of Electronics and Communication Engineering, The LNM Institute Of Information Technology, Jaipur, India.

Background—Fragmented QRS (f-QRS) has been proven to be an efficient bio-marker for several diseases including remote and acute myocardial infarction, cardiac sarcoidosis, non-ischemic cardiomyopathy etc. It has also been shown to have higher sensitivity and/or specificity values than the conventional markers (e.g. Q-wave, ST-elevation etc.) which may even regress or disappear with time. Patients with such diseases have to undergo expensive and sometimes invasive tests for diagnosis. Automated detection of f-QRS followed by identification of its various morphologies in addition to the conventional ECG features (e.g. P, QRS, T amplitude and duration etc.) extraction will lead to a more reliable diagnosis, therapy and disease prognosis than the state-of-the-art approaches and thereby will be of significant clinical importance for both hospital-based and emerging remote health monitoring environments as well as for implanted ICD devices.

Methods and Results—An automated algorithm for detection of f-QRS from the ECG and identification of its various morphologies is proposed in this work which, to the best of our knowledge, is the first work of its kind. Using our recently proposed Time-Domain Morphology and Gradient (TDMG)-based ECG feature extraction algorithm, the QRS complex is extracted and Discrete wavelet transform (DWT) with one level of decomposition, using ‘Haar’ wavelet, is applied on it to detect the presence of fragmentation. Detailed DWT coefficients were observed to hypothesize the postulates of detection of all types of morphologies as reported in the literature. To model and verify the algorithm PhysioNet’s PTB database was used. 40 patients were randomly selected from the database and their ECG was examined by two experienced cardiologists and the results were compared with those obtained from the algorithm. 31 out of 40 patients were considered appropriate for comparison by two cardiologists and it is shown that 334 out of 372 (89.8%) leads from chosen 31 patients comply favorably with our proposed algorithm. The sensitivity and specificity values obtained for the detection of f-QRS were 0.897 and 0.899 respectively.

Conclusions—Automation will speed-up the detection of fragmentation reducing the human error involved and will allow it to be implemented for hospital-based remote monitoring and ICD devices.

Key Words: Electrocardiography, fragmented QRS (f-QRS), wavelet transform

Recently in last 5 years fragmented QRS (f-QRS) has gained clinical significance in diagnosis of various Cardiac disorders including remote and acute myocardial infarction, cardiac sarcoidosis, non-ST-elevation myocardial infarction, ventricular aneurysm etc. [1-15]. These studies have shown that f-QRS complexes can be an important bio-maker for detection of several diseases and has resulted in higher sensitivity and/or specificity than other conventional markers e.g. Q-wave, ST-elevation etc. [1-15]. However, despite of

enormous diagnosis significance cardiologists often disregard or do not report fragmentation in most of the cases except those of bundle branch block (BBB). Therefore, automatic detection and identification of morphologies of fragmented QRS will precisely report on all the cases and may help in finding correlations of potential clinical significance by analyzing hundreds of tracings and hence, will facilitate its widespread clinical acceptance, adaptation and application.

* Author for correspondence (amit_acharyya@iith.ac.in)

Table 1 – Cardiologic disorders along with their conventional marker and limitations

Cardiologic Disorder	Conventional Marker	Remarks
Acute and remote Myocardial Infarction with Coronary Artery Disease (CAD)	Acute ST-elevation, Q-wave	After an acute MI resolves repolarization abnormalities stabilize and only Q-wave then remains as a marker of MI. Q-waves regress or even disappear with time and there is no specific sign of a non Q-wave MI non-ST elevation MI ^{2,4} .
Bundle branch block, premature ventricular complexes and paced rhythm	QRS \geq 120ms	No ECG Diagnosis prior MI scar without the presence of Q wave has been defined. Patients have to undergo expensive diagnosis test e.g. SPECT test, echocardiography etc ⁵ .
Left ventricular aneurysm with QRS \leq 120ms	ST elevation with presence of prominent R wave in aVR	Low specificity as ST-segment elevation are present in many cardiac diseases and Goldberger's sign of prominent R also has low sensitivity ³ .
Cardiac sarcoidosis	No current marker	Diagnosed by myocardial biopsy, cardiac magnetic resonance imaging with gadolinium-delayed enhancement images, echocardiography. Myocardial biopsy is invasive and has low sensitivity, there is no single diagnostic test but a combination clinical data and investigation of CMR with GDE are used for diagnosis ⁹ .
Non-ST-elevation myocardial infarction (NSTEMI)	Ischemic T-waves, ST-segment depression, microvolt T-wave alternans, late potentials on the signal-averaged ECG, pathologic Q waves	Sensitivity and specificity of f-QRS has been found to be higher than Ischemic T-waves. For other bio-markers their correlation with the exact anatomic location of the culprit lesion is not very high ⁸ .

In general, the diagnostic information is obtained from standard 12-lead ECG using the conventional biomarkers e.g. P, Q, R, S waves, their duration and peaks, ST elevation/depression, PT interval and (non)inverted T wave [16]. However, there are certain diseases e.g. cardiac sarcoidosis, myocardial infarction etc. [2-5,9] which cannot be detected by these conventional bio-markers e.g. Q wave, ST elevation/depression, PT interval etc. Patients suffering from these diseases may have to undergo several invasive or non-invasive tests for reliable diagnosis which may be unaffordable [2-5,9]. f-QRS in this context has been found to be a marker for aforementioned diseases and its occurrence in standard 12-lead makes it an inexpensive and easily available tool for diagnosis. Table 1 provides information on diseases which have been found to have high sensitivity and/or specificity values for diagnosis using f-QRS [2-5,8,9] along with the conventional markers/tests that are used to diagnose these diseases and their limitations. Computerized ECG interpretation and feature extraction are being successfully used in a hospital-based environment [17]. Furthermore, significant prevalence of cardiovascular diseases throughout the world resulted in emerging remote health monitoring system which also demands automated, low complexity feature extraction algorithms ported into sophisticated mobile devices or within onboard sensors processing modules [16,18,19]. An automated algorithm can find direct applications in remote health monitoring. It has been found that f-QRS can be used as selection criteria for

implantation of ICD devices [20,21]. A long-term monitoring is required for this purpose and an automated system will considerably reduce the effort required for verification of the signals. However, to the best of our knowledge f-QRS detection and identification of its various morphologies have not been automated and implemented in practice. Here we propose an automated algorithm for f-QRS detection and morphology identification.

METHOD

Fig. 1 presents the procedure followed in the proposed method. The raw ECG signal is passed through a preprocessing module comprising of baseline wandering removal and denoising which will be discussed in subsection II. Then, out of existing ECG feature extraction technique [16,19,22-25] our recently proposed Time Domain Morphology and Gradient (TDMG) based algorithm [16] is applied to extract the QRS complex which is interpolated next and fed as an input to the fragmentation detection and identification (FDMI) module. We skip here the detailed discussion on TDMG algorithm. Interested readers may consult [16] for the details. If fragmentation is detected its morphology is then identified. This FDMI module will be discussed next. Online QRS detection has been investigated by several researchers [22-25] and hence the availability of an accurately detected QRS can be safely assumed. In this work, DWT has been applied using 'Haar' wavelet. Since, Haar wavelet is discontinuous and anti-symmetric [35], it is suitable for discontinuity

* Author for correspondence (amit_acharyya@iith.ac.in)

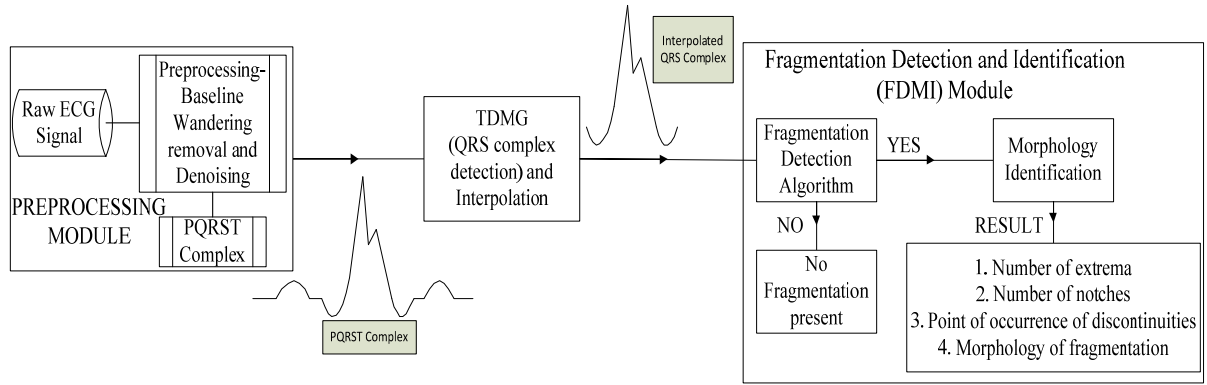


Fig. 1- Procedure followed for the detection and identification of fragmentation in QRS of ECG signal.

and edge detection [35]. Moreover, due to its low computational complexity and power consumption, it is suitable for remote health monitoring applications [19]. Hence, Haar is used in this investigation. Detailed discussion on the “Haar” wavelet based transform seems to be out-of-scope of this present paper. However interested readers are requested to consult the Section-III of reference [19] to know about it in more detail.

I. FDMI module

This section has been further subdivided into two subsections viz. Fragmentation detection and Morphology identification.

A. Fragmentation Detection

The detailed DWT coefficients behave in a particular manner when a discontinuity* is encountered. A peak or nadir in any signal can be detected by the zero crossing of the wavelet transform. This technique has been previously used to detect QRS complexes of ECG [23]. In this subsection we explain this behavior with the help of Fig. 2. Consider a line segment with positive slope joining two points and the corresponding bar plot of detailed DWT coefficient as shown in Fig. 2A, it can be seen that the coefficient is negative for an increasing segment. Fig. 2B shows a line segment with negative slope and the corresponding bar plot of detailed DWT coefficient which in this case is positive. In Fig. 2C a set of points have been drawn along with the bar plot of their detailed DWT coefficients. It can be inferred from Fig. 2A-C that an increasing part of the curve results in negative and decreasing part of the curve results in positive detailed DWT coefficients respectively. It should also be noted that the magnitude of the coefficients depend on the slope of the tangent at that point. Greater the slope greater is the magnitude of the

coefficient. Whenever a local extremum appears there is a transition in the sign of the detailed coefficient depending on the presence of a maxima or minima. We confirm this hypothesis with Fig. 2D in which both the extrema are identified i.e. first the maxima and then the minima. This phenomenon has been used in modeling and designing of the proposed fragmentation detection algorithm. The notches [1-15] that occur in the QRS complex are identified as frequent changes in the sign of detailed coefficients and a peak is identified as sudden change in sign with a constant follow up of the coefficients with same sign.

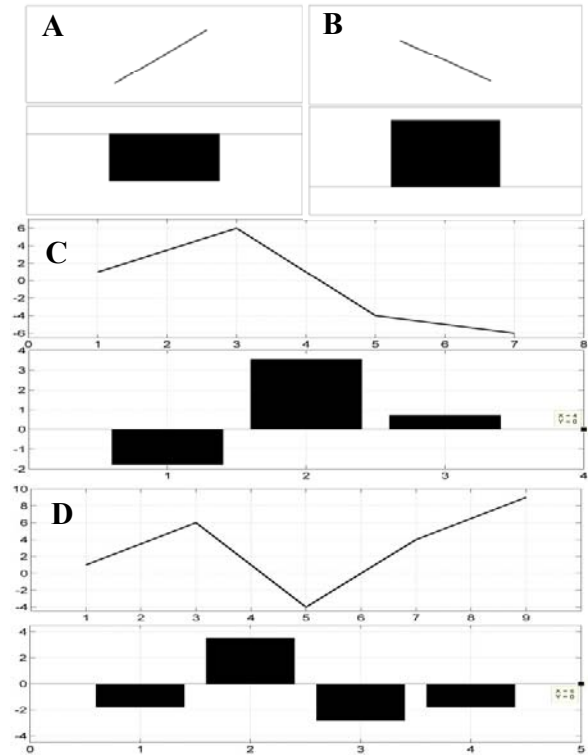


Fig. 2- Explanation of patterns observed on occurrence of a discontinuity.

* Discontinuity is discussed later in this subsection

* Author for correspondence (amit_acharyya@iith.ac.in)

Table 2 – Rules for identification of discontinuities.

PATTERN		DESCRIPTION [†]		POINT OF OCCURRENCE
NOTCH				
		A1 — $a > 0; b < 0; c > 0; d > 0$ $k = k + 2$	A3 — $a < 0; b > 0; c < 0; d < 0$ $k = k + 2$	A3 and A4 Peak — $a + b$ Nadir — $b + c$
		A2 — $a > 0; b < 0; c > 0; d < 0$ $ b \neq c ; k = k + 2$ If $ b > c $ then C6	A4 — $a < 0; b > 0; c < 0; d > 0$ $ b \neq c ; k = k + 2$ If $ b > c $ then C5	A1 and A2 Peak — $b + c$ Nadir — $a + b$
NOTCH				
		B1 — $a > 0; b < 0; c < 0; d > 0$ $\max(b , c) < d ;$ $k = k + 3$ If $\max(b , c) > d $ then C4	B2 — $a < 0; b > 0; c > 0; d < 0$ $\max(b , c) < d $ $k = k + 3$ If $\max(b , c) > d $ then C3	B1 Peak — $c + d$ Nadir — $a + b$ B2 Peak — $a + b$ Nadir — $c + d$
EXTREMA				
		C1 — $a < 0; b > 0; c > 0; d > 0$ $k = k + 3$	C2 — $a > 0; b < 0; c < 0; d < 0$ $k = k + 3$	C1, C2, C3, C4, C5, C6 Peak or Nadir — $a + b$
		C3 — $a < 0; b > 0; c > 0$ $k = k + 2$	C4 — $a > 0; b < 0; c < 0$ $k = k + 2$	
		C5 — $a < 0; b > 0$ $k = k + 1$	C6 — $a > 0; b < 0$ $k = k + 1$	

[†]Pointer 'k' initially starts at 'a'. 'a', 'b', 'c' and 'd' are consecutive points on the bar plot of discrete coefficients and denote the corresponding boxes. Incrementing 'k' shifts it from box 'a' to box 'b'.

#|l| — denotes magnitude of the detailed coefficient at a particular point.

[†]Pointer 'k' initially starts at 'a'. 'a', 'b', 'c' and 'd' are consecutive points on the bar plot of discrete coefficients and denote the corresponding boxes. Incrementing 'k' shifts it from box 'a' to box 'b'.

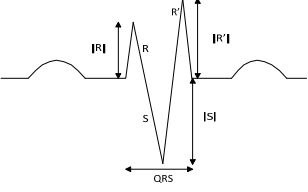
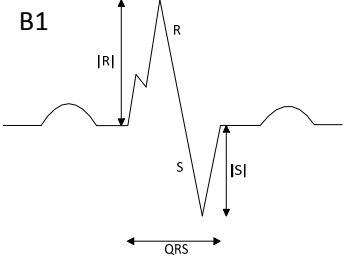
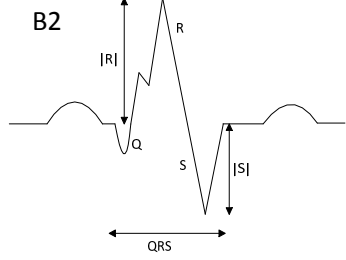
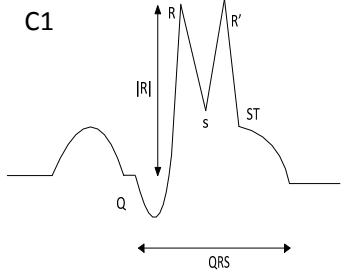
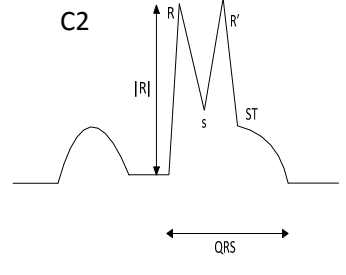
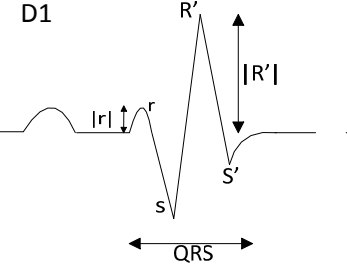
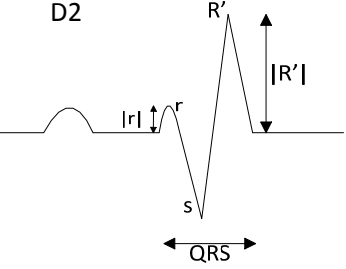
[#]1.1 — denotes magnitude of the detailed coefficient at a particular point.

In Fig. 2, bar plots of detailed DWT coefficients of interpolated QRS complex are plotted and rules for identifying extrema and notches are formulated by observing and correlating the patterns occurring in the QRS complex and detailed coefficients. It is to be noted that the bars may not seem to align because the scale of the x-axis of the wave and the bar plot of detailed discrete wavelet transform (DWT) coefficients are different. When DWT is applied the number of detailed coefficients obtained is half the number of samples on which DWT was applied. The main purpose of using Fig. 2 is to show the behavior of detailed coefficients when increasing or decreasing part of wave is encountered. In Fig. 2C, the wave has 7 samples and the total number of detailed coefficients are 4,

however, the 4th coefficient is zero. Similarly, in Fig. 2D, the number of samples are 9 and coefficients are 5, however, the last coefficient is zero which are indicated in Fig. 2. Detailed discussion on the DWT can be found in [19]. With the help of few patients the criteria in Table 2 were hypothesized and were then iteratively refined by applying them on leads of 40 subjects such that the mentioned criteria accurately and reliably captured all sorts of discontinuities occurring in the QRS complexes. Table 2 presents the rules framed for detection of local extrema and notches. Algorithm starts evaluating the QRS complex from left-most side of the bar plot and proceeds to the right. While traversing through the coefficients patterns are recognized and if any pattern matches to those mentioned in Table 2 the

* Author for correspondence (amit_acharyya@iith.ac.in)

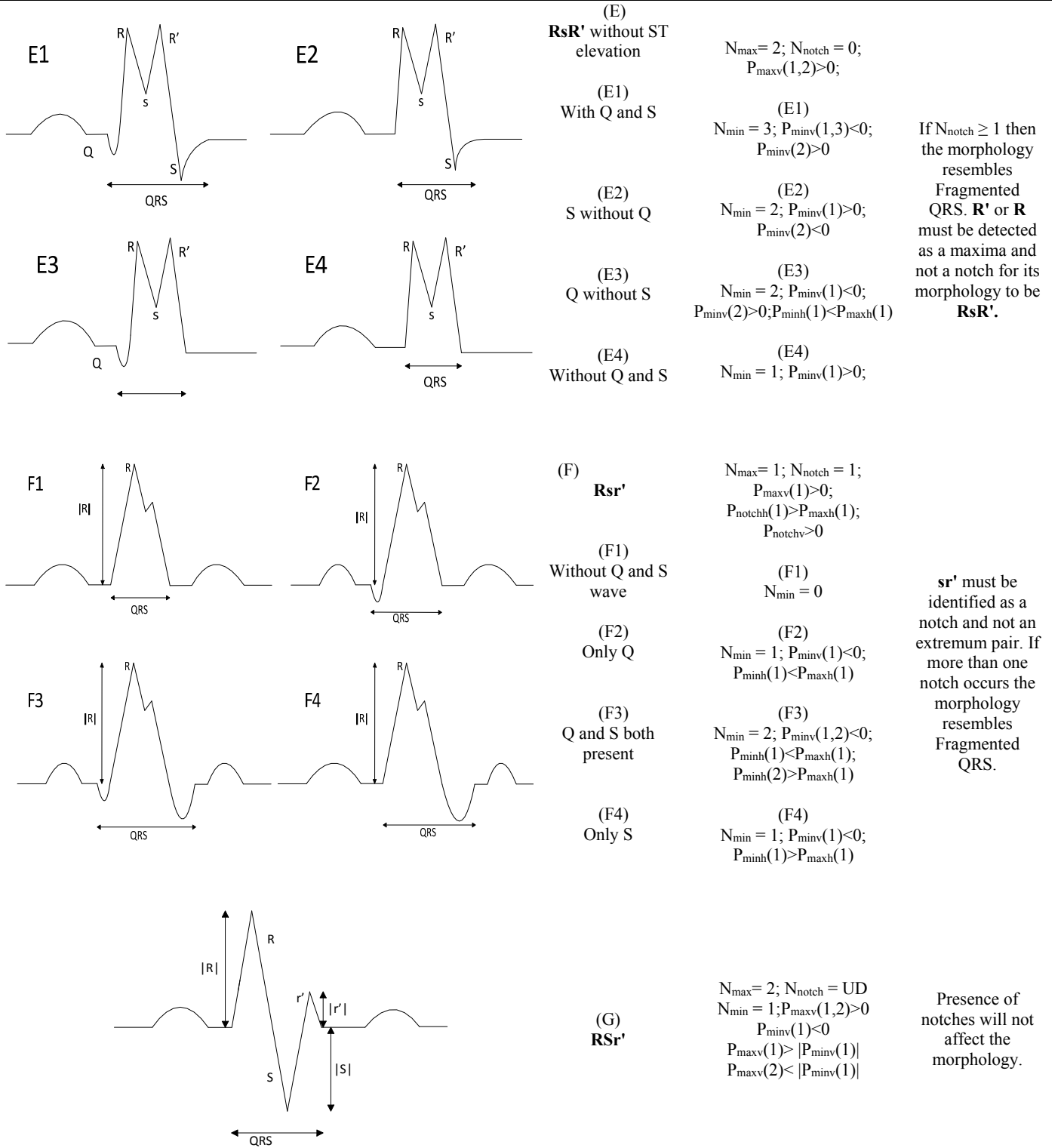
Table 3A - QRS ≤ 120 ms (f-QRS)

Morphology	Name	Criteria	Conflict
	(A) rSr'	(A) $\max(P_{maxv}(1,2)) < P_{minv}(1) $ $N_{max} = 2$ $N_{min} = 1$ $P_{maxv}(1,2) > 0$ $P_{minv}(1) < 0$ $N_{notch} = NF^\dagger$	When this morphology is encountered, the presence of notches on R, R' or S wave will not lead it to be termed as fragmented QRS.
 	(B) Notched R (rsR') (B1) Without Q (B2) With Q	$N_{max} = 1; N_{notch} = 1$ $P_{maxv}(1) > 0; P_{notchv}(1) > 0$ $P_{notchh}(1) < P_{maxh}(1)$ (B1) $N_{min} = 1; P_{minv}(1) < 0$ (B2) $N_{min} = 2; P_{minv}(1,2) < 0$	when $N_{notch} > 1$ then the morphology resembles Fragmented QRS.
 	(C) RsR' with ST elevation (C1) With Q (C2) Without Q	$N_{max} = 2; N_{notch} = 0;$ $P_{maxv}(1,2) > 0;$ End of QRS complex must lie above horizontal axis. (C1) $N_{min} = 2; P_{minv}(1) < 0;$ $P_{minv}(2) > 0$ (C2) $N_{min} = 1; P_{minv}(1) > 0$	Case may arise when sR' is identified as a notch instead of a minima-maxima pair. Then all the cases arising are captured by morphology (F). For an extremum to be R it has to be identified as a maximum.
 	(D) rSR' (D1) With S' (D2) Without S'	$N_{max} = 2; P_{maxv}(1,2) > 0;$ $P_{maxh}(1) < P_{minh}(1)$ (D1) $N_{min} = 2; P_{minv}(1,2) < 0$ (D2) $N_{min} = 1; P_{minv}(1) < 0;$ $P_{maxv}(1) < P_{minv}(1);$ $P_{minv}(1) < P_{maxv}(2);$	Presence of notches will not affect the morphology.

$^\dagger NF$ — Number and presence of notches not fixed

N_{max} — Number of maxima; N_{min} — Number of minima; N_{notch} — Number of notch; $P_{maxv}(i)$ — Position at which i^{th} maxima occurs on the vertical axis (magnitude along with sign); $P_{maxh}(i)$ — Position at which i^{th} maxima occurs on the horizontal axis; $P_{minv}(i)$ — Position at which i^{th} minima occur on the vertical axis; $P_{minh}(i)$ — Position at which i^{th} minima occurs on the horizontal axis; $P_{notchv}(i)$ — Position at which i^{th} notch occurs on the vertical axis; $P_{notchh}(i)$ — Position at which i^{th} notch occurs on the horizontal axis

* Author for correspondence (amit_acharyya@iith.ac.in)



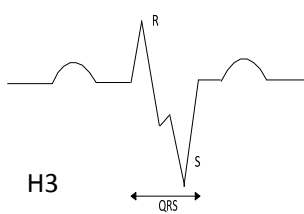
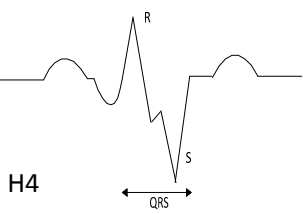
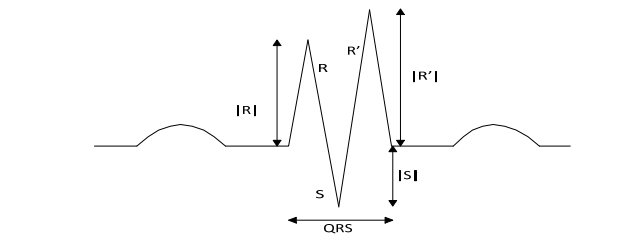
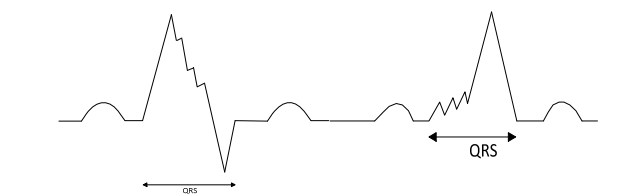
<div> <div>H1</div>  <div>H3</div> </div> <div> <div>H2</div>  <div>H4</div> </div>	<div>(H)</div> <div>Notched S</div> <div>(H1 and H3)</div> <div>Notch in downstroke and upstroke of S wave. Q not present</div> <div>(H2 and H4)</div> <div>Notch in downstroke and upstroke of S wave. Q present.</div> <div>(H5 and H6)</div> <div>If notch is detected as extremum pair in any of the cases.</div>	<div>(H1 and H3)</div> <div> $N_{max} = 1; N_{notch} = 1;$ $N_{min} = 1; P_{minv}(1) < 0$ $P_{maxv}(1) > 0; P_{notchv} < 0$ $P_{notchh}(1) > P_{maxh}(1);$ </div> <div>(H2 and H4)</div> <div> $N_{max} = 1; N_{notch} = 1;$ $N_{min} = 2; P_{minv}(1,2) < 0$ $P_{maxv}(1) > 0; P_{notchv} < 0$ $P_{notchh}(1) > P_{maxh}(1);$ </div> <div>(H5)</div> <div> $N_{max} = 2; N_{min} = 2;$ $N_{notch} = 1;$ $P_{maxv}(1) > 0; P_{maxv}(2) < 0$ $P_{minv}(1,2) < 0$ </div> <div>(H6)</div> <div> $N_{max} = 2; N_{min} = 3$ $N_{notch} = 1;$ $P_{maxv}(1) > 0; P_{maxv}(2) < 0$ $P_{minv}(1,2,3) < 0$ </div>	<p>If more than one notch is present then the morphology will be termed as Fragmented QRS. Notch may be discovered as a extremum pair but still the morphology resembles Notched S.</p>
 	<div>(I)</div> <div>RSR'</div> <div>(J)</div> <div>Fragmented QRS</div>	<div>(I)</div> <div> $\min(P_{maxv}(1,2)) > P_{minv}(1)$ $N_{max} = 2; N_{min} = 1$ $P_{maxv}(1,2) > 0$ $P_{minv}(1) < 0$ $N_{notch} = NF$ </div> <div>(J)</div> <div> <p>If none of the aforementioned morphologies are detected and</p> $N_{notch} \geq 1;$ Or $N_{max} \geq 2; N_{min} \geq 2$ </div>	<p>Presence of notch doesn't affect the morphology.</p> <p>Visually identified notch may be detected as an extremum pair. If so, then such morphology will be termed as Fragmented QRS. Notches may occur in R and/or S wave.</p>

Table 3B - QRS ≥ 120 ms (f-wQRS)

Name	Definition	Criteria
Fragmented Bundle Branch Block (f-BBB)	Various RSR' patterns with or without Q wave with >2 R waves (R') or >2 notches in the R wave or >2 notches in downstroke or upstroke of S wave	$N_{max} > 2$ Or At least 3 notches in the positive half plane Or At least 3 notches in the negative half plane
Fragmented Premature Ventricular Complex (f-PVC)	>2 R waves (R') or >2 notches in the downstroke or upstroke of S wave or Only 2 notches in the R with >40ms separation	$N_{max} > 2$ Or At least 3 notches in the negative half plane Or 2 notches in the positive half plane with >40ms delay
Fragmented Paced Rhythms (f-pQRS)	>2 R waves (R') or >2 notches in the downstroke or upstroke of S wave	$N_{max} > 2$ Or At least 3 notches in the negative half plane

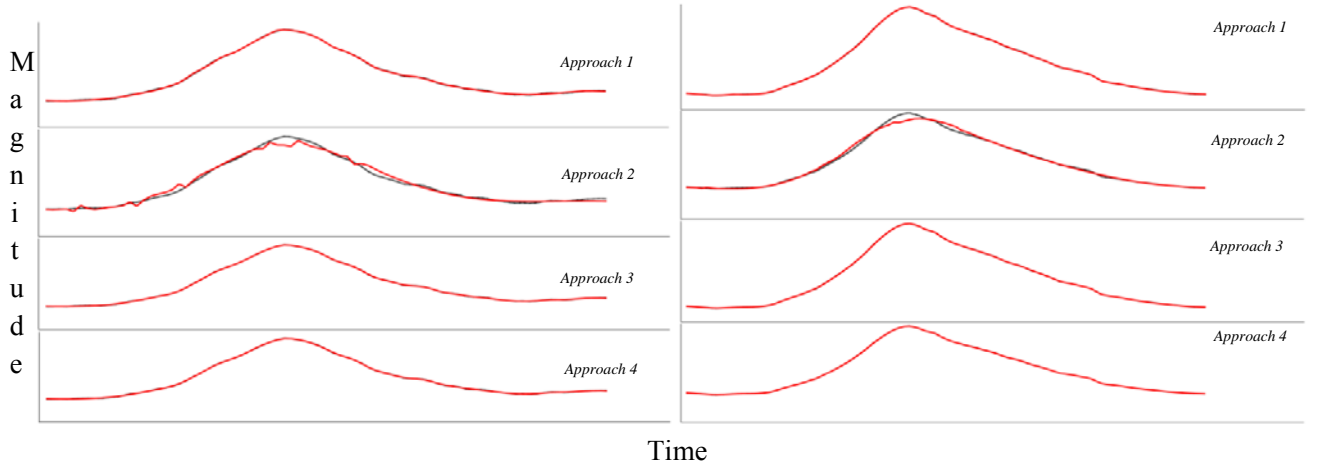


Fig. 3- Two instances in which *Approach 2* was found to be tampering the QRS complex

corresponding discontinuity[‡] is realized and noted. Algorithm pointer (k) pointing at a particular point of the QRS complex is incremented according to presence and type of discontinuity encountered. If a discontinuity is spotted it is identified and pointer increments as per the mentioned rule (Table 2) or else it increments by one. For example, in pattern A1 as shown in Table 2, there are two consecutive sign changes in the values of detailed coefficients which can be attributed to the occurrence of an local extremum pair in close proximity and hence can be assumed to be a notch. Similarly, in pattern A2 there are three consecutive sign changes implying there are three extrema and the one that is identified as a notch depends on the magnitude of the detailed coefficient, the other is identified as an extremum. Other patterns for the identification of notch and extremum can be interpreted in a similar fashion as mentioned in Table 2.

B. Morphology Identification

There exist six fundamental morphologies of fragmented QRS and several other variations of **RSR'** patterns which were exemplified in the literature [1-15]. Apart from those mentioned, for the sake of completion we have attempted to encompass all the possible variations in **RSR'** patterns, for example, some morphologies were found to have a Q-wave which was not reported in the six fundamental morphology as shown in B2, C1 etc. in Table 3. However, all the originally mentioned morphologies identified as fragmented QRS have been included. Table 3 summarizes and states the criteria for identification of the corresponding morphologies. Table 3A presents all

the 10 morphologies that were quantified for $QRS \leq 120\text{ms}$ and Table 3B presents the criterion for the identification of morphologies with $QRS \geq 120\text{ms}$ which are generally encountered in practice and appeared in literature. The criterion of identification preferably starts once the number of maxima, minima and notch, the point of occurrence i.e. positive or negative side of the reference axis, sequence of occurrence and height and depth of R and S waves respectively have been obtained from the fragmentation detection step. **We have attempted to maintain a clear difference between an extremum pair and a notch. Morphologies with 2 R waves (R') viz. A, C, E and I have been considered to be dominating over the presence of notches so as to prevent such morphologies to be identified as Fragmented QRS. Notched S morphology where the notch is being identified as an extremum pair was encountered,** this case has also been taken into account. Similar morphologies for **R** waves exist and has been identified as **RsR'** patterns. These criteria have been formulated based on the appearance of the QRS complex and have been assigned to morphologies such that each one can be identified distinctly i.e. criteria assigned to morphologies can distinctively identify them without any conflict.

II. Preprocessing and Feature Extraction

Wavelet based techniques have been implemented for low power and low complexity applications [19]. Several wavelet transform based artifact removal algorithms have been proposed in the literature [27-30]. However, there exists no clear demarcation upon the performance of these denoising techniques for comparison. Hence, all these techniques were employed and the denoised signals were visually observed.

[‡]discontinuity in general refers to any local extrema considered i.e. notch, maxima or minima

* Author for correspondence (amit_acharyya@iith.ac.in)

Discrete wavelet transform (DWT) has been used to remove the baseline wandering and have tested four different variants of wavelet transform to denoise the raw ECG signal. **Baseline wandering removal using DWT [27] involves decomposition down to level 9 and wavelet filter used is Symlet 10.** The denoising approaches are as follows:

Approach 1: Denoising and artifact removal using DWT [28]. Decomposition down to level 3. Wavelet filter used was Symlet 4.

Approach 2: Denoising and artifact removal using stationary wavelet transform (SWT)[29]. Decomposition down to level 4. Wavelet filter used was Symlet 4. Empirical Bayes posterior median thresholding is used.

Approach 3: Denoising and artifact removal using undecimated wavelet transform (UWT)[30]. Wavelet filters were Daubechies 6. The level of decomposition was self-determined by the code [31]. We used classical standard deviation type of variance estimator and hard thresholding.

Approach 4: Denoising and artifact removal using translation invariant wavelet transform (TIWT)[27]. Wavelet filters used were Symlet 8. Hard thresholding was used and level of decomposition was self-determined by the code [32].

It was found that *Approach 2* and in very rare cases *Approach 1* were tampering with the QRS complex. Fig.3 shows two instances taken from two different subjects where the tampering with the original signal was found while using *Approach 2* (SWT), the denoised signal is plotted against the baseline wandering removed signal which was initially verified as not tampering with the signal. It can be seen that notches have been introduced even though the original complex did not have one; other denoising techniques have smoothly retraced the original QRS complex. This visual inspection was done for more than 40 subjects and in rare instances DWT was also found to tamper the complex but none such cases were encountered for *Approach 3* and *4*. *Approach 3* (UWT) and *Approach 4* (TIWT) were satisfactorily denoising the signals. For designing and verification of the algorithm *Approach 4* was adopted as this denoising technique was applied and verified with signals obtained at higher sampling frequencies[26] and satisfactory results were obtained.

The proposed algorithm was implemented on MATLAB (ver. 7.10.0-2010a). The appendix provides the MATLAB code snippet for the implementation of the baseline wandering and denoising techniques.

EXPERIMENTS AND RESULTS

This section has been divided into the following subsections. Subsection I presents the experimental setup, subsection II discusses the case studies to understand the working principle of the algorithm, section III presents the evaluation methods used to measure the performance of the algorithm in terms of accuracy and subsection IV presents the results.

I. Experimental Setup

PTB database (PTBDB) [33,34] from PhysioNet has been used for the designing and verification of the proposed algorithm. PTBDB is an unprocessed or raw 15 lead database comprising of conventional 12 leads and 3 orthogonal Frank leads digitized simultaneously at sampling frequency of 1 kHz and captured at the standard speed of 25mm/s and 10mm/mV with grid intervals being 0.2s and 0.5mV. The database was categorized on the basis of cardiac disorders reported and ECG of patients from various categories was used for designing and modeling of the algorithm. **PTBDB consists of patients belonging to various diagnostic classes viz. myocardial infarction, cardiomyopathy/heart failure, bundle branch block, dysrhythmia, myocardial hypertrophy, Valvular heart disease, myocarditis, healthy controls and other miscellaneous** [33,34]. A high sampling rate is desired to capture the occurrence of high frequency notches in QRS complexes. A simple linear interpolation is then applied on the preprocessed signal to further increase the number of samples so that the detailed coefficients obtained after applying DWT can accurately detect all discontinuities (local extrema and notches) as DWT diminishes the time resolution by a factor of 2. Eq. (1) shows the methodology adopted for interpolation.

$$Y_{interpolated} = \frac{Y_k + Y_{k+1}}{2} \quad (1)$$

A mean was calculated for every two consecutive samples and was inserted in between them thus increasing the total number of samples. Interpolation in this manner is extremely simple and does not affect the points of extrema. Requirement of interpolation is based on observational interpretations during the designing of the algorithm. Upon interpolation it was observed that the detailed coefficients were found to capture all the

* Author for correspondence (amit_acharyya@iith.ac.in)

discontinuities without fail. The MATLAB code snippet for the implementation of linear interpolation and DWT can be found in the appendix.

II. Case Studies

The outputs obtained from the algorithm are the number of extrema points (maxima and minima), notches, time instants at which they occur, magnitude of extrema, the occurrence on the lower or upper half of the magnitude-time plane and the morphology of fragmentation encountered. In this subsection, we discuss 8 different cases and the output obtained from the algorithm for them which are intended to show the working principle of our proposed algorithm. These complexes were randomly selected from the large database avoiding the selections where similar morphologies were selected. Fig.4.1-4.8 shows the plot of these cases with part 'a' of the plot showing the interpolated QRS complex and part 'b' of the plot showing the bar plot of the detailed coefficients obtained after applying DWT. Notches and extrema are denoted by circle and rectangle respectively. The following cases correspond to the QRS complexes shown in Fig.4. This case study provides insight into the working of the algorithm and will help in the reproduction of the work. Rules mentioned in Table 2 have been used to detect the discontinuities and criteria mentioned in Table 3 have been used to identify the morphology.

Case 1: This case is an example of Notched R (rsR') morphology. Number of maxima, minima and notches are 1, 2 and 1 respectively. On examining Fig.4.1a it can be seen that a minima (<0) is encountered first followed by a notch (>0), maxima (>0) and a second minima (<0).

Case 2: This case is an example of RsR' without ST elevation. Number of maxima, minima and notches are 2, 2 and 0 respectively. In Fig.4.2b, a maxima (>0) is encountered first followed by minima (>0), maxima (>0) and minima (<0).

Case 3: This case is an example of Rsr'. Number of maxima, minima and notches are 1, 2 and 1 respectively. In Fig.4.3b, a minima (<0) is encountered first followed by maxima (>0), notch (>0) and minima (<0).

Case 4: This case is an example of Notched S. Number of maxima, minima and notches are 2, 2 and 0 respectively. In Fig.4.4b, a maxima (>0) is encountered

first followed by minima (<0), maxima (<0) and minima (<0).

Case 5: This case is an example of rSr'. Number of maxima, minima and notches are 2, 1 and 1 respectively. In Fig.4.5b, a maxima (>0) is encountered first followed by notch (>0), minima (<0) and maxima (<0).

Case 6: This case is an example of Fragmented QRS. Number of maxima, minima and notches are 2, 3 and 0 respectively. In Fig.4.6b, a minima (<0) is encountered first followed by maxima (>0), minima (<0), maxima (>0) and minima (<0).

Case 7: This case is an example of Fragmented QRS. Number of maxima, minima and notches are 3, 4 and 0 respectively. In Fig.4.7b, a minima (<0) is encountered first followed by maxima (>0), minima (>0), maxima (>0), minima (>0), maxima (>0) and minima (<0).

Case 8: The length of QRS is more than 120ms ($QRS \geq 120ms$). This case resulted in f-BBB with 3 or more R waves (R'). Number of maxima, minima and notches are 3, 2 and 1 respectively. In Fig.4.8b, a maxima (>0) is encountered first followed by minima (<0), maxima (>0), notch (>0), minima (>0), maxima (>0).

III. Evaluation Criteria

Forty patients were selected at random from the database, the QRS complexes were extracted using the TDMG feature extraction algorithm and were examined by the cardiologists. Out of 40 patients 9 patients were removed from the study pertaining to the bad quality of their ECG as per the suggestion of the cardiologists. The remaining QRS complexes were then independently examined by the two cardiologists in a blinded fashion and finally a consensus was reached to produce the final result which will be hereby referred as cardiologist's status (CS). The measurements obtained from the cardiologists are assumed to be the gold standard. The QRS complexes were then input to the Fragmentation Detection Algorithm (FDA) and the results obtained were compared with CS and sensitivity and specificity values were calculated. The following will discuss the test results and test nature:

True positive: The cardiologists detected fragmentation in a particular lead of the patient and the algorithm reported correctly.

* Author for correspondence (amit_acharyya@iith.ac.in)

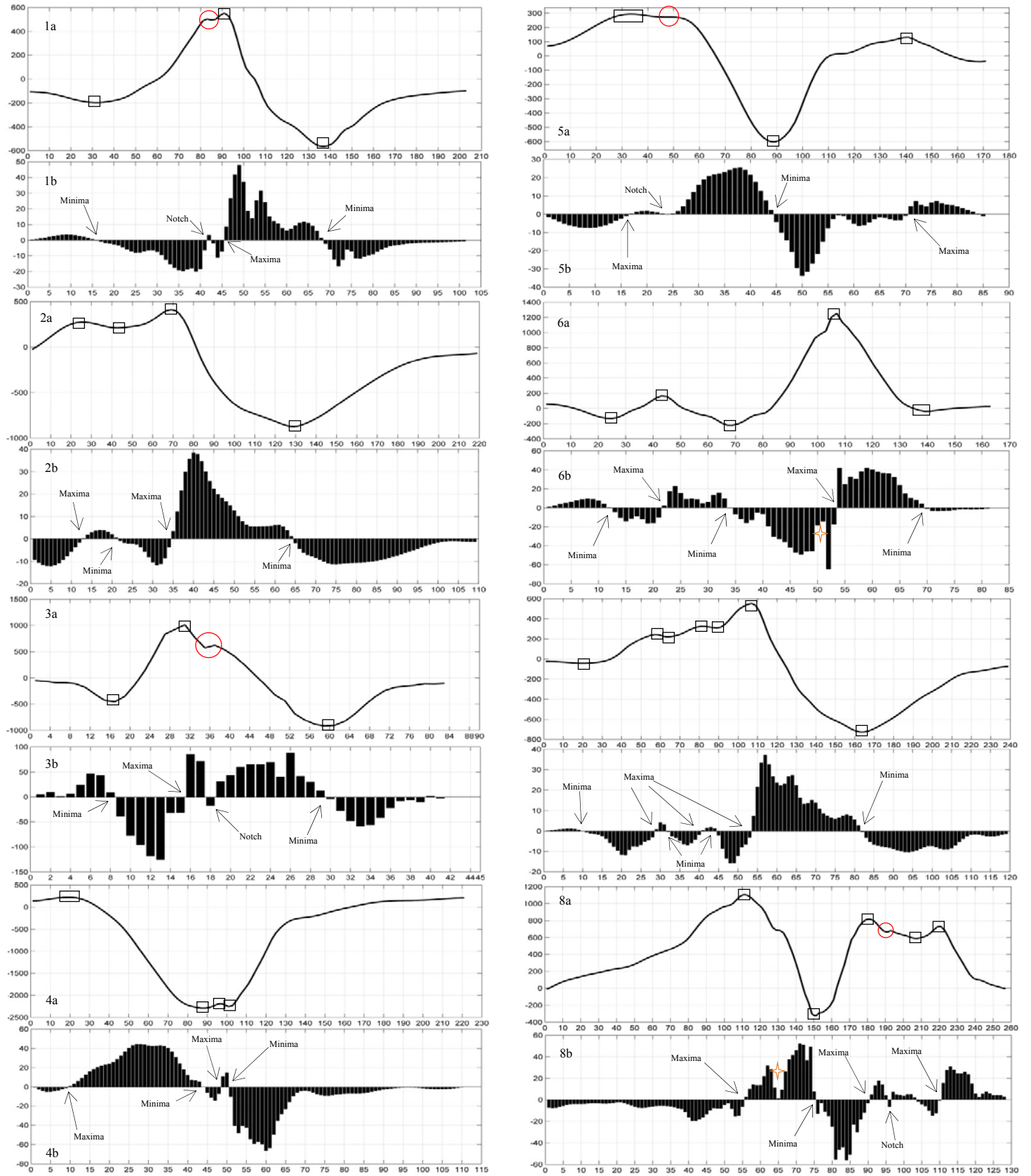


Fig. 4- Eight different morphologies 1-8 comprising of an interpolated plot along with bar plot of its detailed coefficients obtained after applying DWT. Square boxes denote extrema and circle denotes notch. 4-point star shows the sudden changes in gradient of the wave, however, these do not lead to discontinuity. This star has been used to demonstrate the sensitivity of the algorithm in capturing gradients of the wave encountered.

* Author for correspondence (amit_acharyya@iith.ac.in)

False positive: The cardiologists did not detect fragmentation but the algorithm reported the presence of fragmentation in a particular lead.

True negative: The cardiologists did not detect fragmentation and the algorithm reported correctly.

False negative: The cardiologists detected fragmentation in a particular lead but the algorithm could not detect.

The sensitivity and specificity was calculated using the following equations:

$$\text{Sensitivity} = \frac{\text{True positives}}{\text{True positives} + \text{False negatives}} \quad (2)$$

$$\text{Specificity} = \frac{\text{True negatives}}{\text{True negatives} + \text{False positives}} \quad (3)$$

IV. Experimental Results

The QRS complexes obtained from TDMG were evaluated by two experienced cardiologists and were simultaneously used to obtain results from the algorithm. From 372 leads (31 patients) selected i.e. only 12-lead ECG of 31 patients and not the Frank leads, the results of 89.8% i.e. 334 leads from FDA complied with that of CS. The sensitivity and specificity values obtained were 0.897 and 0.899 respectively. Since, cardiologists are often interested in fragmentation in the BBB subjects, out of randomly selected 31 patients 5 patients belonged to BBB and the sensitivity and specificity were found to be 0.932 and 0.933 respectively. It is to be noted that in this paper we have evaluated the presence or absence of fragmentation at a lead level rather than patient level which is usually the case in the literature. It is important that the algorithm detects fragmentation correctly in every lead of the patient as well identifies its various morphologies. The sensitivity and specificity values were obtained for the presence or absence of fragmentation and not for the morphology obtained by the algorithm and cardiologists. We haven't found any work which standardizes the morphologies of fragmentation for the common agreement and hence, we have avoided the evaluation of the morphological results obtained from the algorithm.

DISCUSSION

From Fig.4.1-4.8 we can see that whenever the gradient of the wave is high the magnitude of the detailed

coefficients is more. Sensitivity of the algorithm can be estimated from the fact that it not only captures the formation of an extremum pair but also sudden changes in gradient which did not result in an extremum pair e.g. in Fig.4.6 and Fig.4.8, a sudden gradient change before the occurrence of final maxima (Fig.4.6b) and after the 1st maxima (Fig.4.8b) can be seen (denoted by a 4-point star in orange color) with the magnitude of detailed coefficients suddenly decreasing and then increasing. This highlights the sensitivity of the detailed coefficients to sudden changes in the ECG and hence it is important to denoise the ECG before applying FDA algorithm or else a noisy part in the QRS complex may be detected as a notch, which upon denoising may not be present. Hence, baseline wandering removal and denoising is required for correct detection of morphology of fragmented QRS.

Sampling rate plays an important role in capturing fragmentation. We have observed that sampling rate of 2 kHz will be appropriate for the algorithm implementation. This can be deduced from the role played by interpolation to double the number of samples as the sampling rate of PTB database is 1 kHz. Significance of number of samples can be seen from Fig. 5 A-D (notches have been denoted by circle in red color). Left half of the figure (1a and 1b) shows plot of interpolated QRS along with bar plot of detailed coefficients. Right half shows the figure (2a and 2b) of original QRS along with the bar plot of its detailed coefficients. All the four figures show that on increasing the number of samples undetectable notches can also be identified. This has been our main motivation behind interpolating. A notch which is detectable will only get elongated or may get converted to an extremum pair; this can be taken care with the help of criteria and postulates for morphology realization and identification respectively but an undetectable notch will result in wrong determination of the number of notches and hence the morphology which may lead to wrong diagnosis. Fig.5A was identified by the algorithm as notched S, 5B as Rsr', 5C as f-QRS and 5D as rSR'.

When pattern similar to Table 2, A1 and A3 are encountered, it unfailingly denotes presence of notch but when patterns like A2 and A4 are encountered it becomes difficult to interpret whether such a pattern should be treated as a notch or an extremum pair. Fig. 5 B1 (a and b) shows a similar case. In the absence of magnitude criterion, the maxima would have been identified as a notch and the peak of the notch would have been identified as a maxima.

* Author for correspondence (amit_acharyya@iith.ac.in)

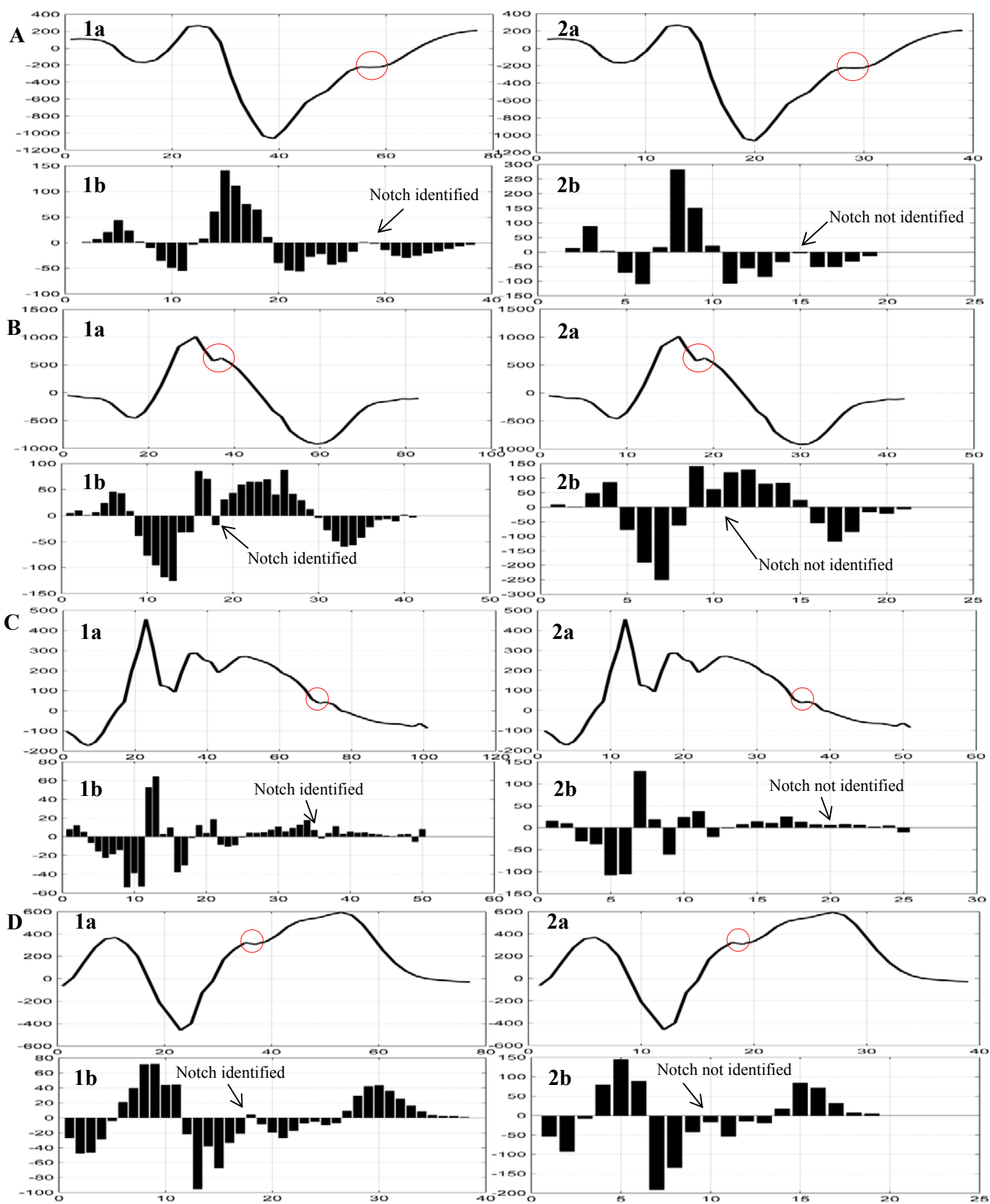


Fig. 5 A-D Significance of Interpolation and magnitude criteria used in Table 2.

* Author for correspondence (amit_acharyya@iith.ac.in)

Properties of the detailed coefficients as explained in Fig. 2 can be used to explain and understand the occurrence of such patterns. Similarly, if the magnitude criteria stated in Table 3, B1 and B2 are spared then on implementation of the algorithm on Fig. 5 C2 (a and b) would have resulted in detection 1st maxima and 2nd minima as two notches which is inaccurate. On iterative refinement of algorithm and evaluating it on more than 40 patients we deemed it necessary to incorporate the magnitude criterion in the postulates. In the designing and modeling phase the method of QRS detection was adopted from the appendix of [35]. For obtaining accurate results from the algorithm it is necessary to input an accurately detected QRS complex. Any extra discontinuity will lead to the identification of some other morphology. In the worst case scenarios, algorithm will identify the morphology as f-QRS leaving no fragmented QRS go undetected.

CONCLUSION

We have introduced a novel approach for detection of discontinuities in the QRS complexes and have verified it using PTBDB. A less complex 'Haar' wavelet was used for low power consumption which can be used in battery operated devices viz. Mobile phone/PDA/Table [19] or battery operated ICD devices. This approach is not signal specific and the method can be applied to any other kind of biomedical signal for detection of its certain important aspects and features. For ECG specific applications, we have formulated the postulates for detection of notches and extrema and have proposed criteria for identification of various morphologies. The significance of denoising techniques and all types of discrepancies encountered have been discussed.

ACKNOWLEDGMENT

This work is partly supported by the DIT, India under the "Cyber Physical Systems Innovation Hub" under Grant number: 13(6)/2010-CC&BT, Dated 1st March 2011 and "IOT for Smarter Healthcare" under Grant No: 13(7)/2012-CC&BT, Dated 25th February, 2013.

APPENDIX

The appendix provides snippet of Matlab codes which will be helpful in reproduction of the work. The part of the code which has considered important and necessary has been provided. Fig. A provides the Matlab code for implementation of denoising techniques and Fig. B

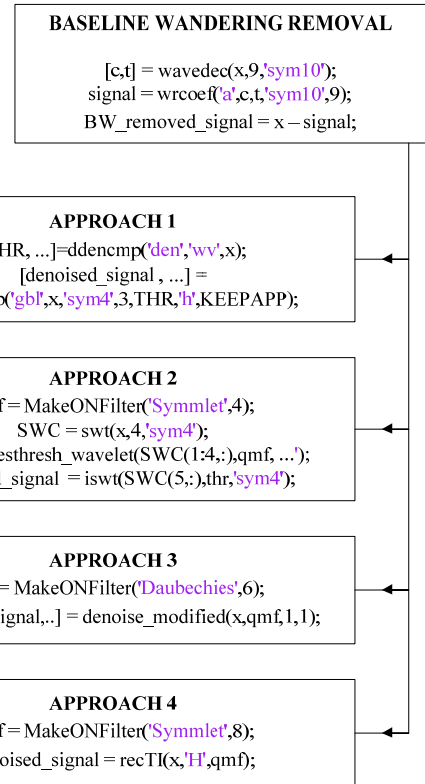


Fig. A- MATLAB code snippet for baseline wandering removal, denoising, interpolation and DWT.

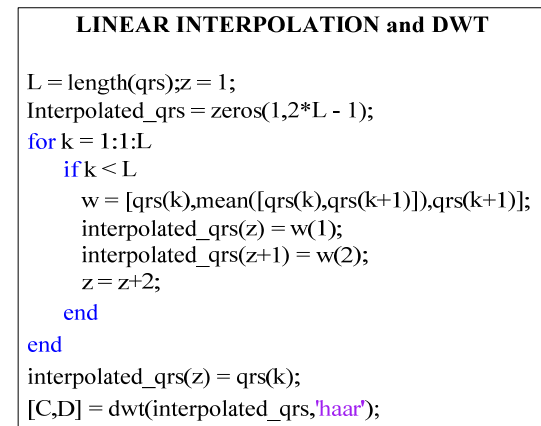


Fig. B- MATLAB code snippet for linear interpolation and DWT.

provides the code for implementation of interpolation and DWT.

REFERENCES

1. Maehara, K., Kokubun, T., Awano, N., Taira, K., Ono, M., Furukawa, T., Shimizu, Y. & Maruyama, Y. 1999 Detection of Abnormal High-Frequency Components in the QRS Complex

* Author for correspondence (amit_acharyya@iith.ac.in)

- by the Wavelet Transform in Patients With Idiopathic Dilated Cardiomyopathy. *Jpn Circ J*. **63**, 25–32. (DOI:10.1253/jcj.63.25)
2. Das, M.K., Khan, B., Jacob, S., Kumar, A. & Mahenthiran, J. 2006 Significance of a Fragmented QRS Complex Versus a Q Wave in Patients With Coronary Artery Disease. *Circulation*. **113**, 2495-2501. (DOI:10.1161/CIRCULATIONAHA.105.595892)
 3. Reddy, C.V.R., Cheriparambill, K., Saul, B., Makan, M., Kassotis, J., Kumar, A. & Das, M.K. 2001 Fragmented Left Sided QRS in Absence of Bundle Branch Block: Sign of Left Ventricular Aneurysm. *J Am Coll Cardiol*. **37**, 1285. (DOI:10.1111/j.1542-474X.2006.00094.x)
 4. Michael, M.A., Masry, H.E., Khan, B.R., & Das, M.K. 2007 Electrocardiographic Signs of Remote Myocardial Infarction. *progvcardiovasc dis*. **50**(3), 198-208. (DOI:10.1016/j.pcad.2007.05.003)
 5. Das, M.K., Suradi, H., Maskoun, W., Michael, M.A., Shen, C., Peng, J., Dandamudi, G. & Mahenthiran, J. 2008 Fragmented Wide QRS on a 12-Lead ECG : A Sign of Myocardial Scar and Poor Prognosis. *Circ Arrhythm Electrophysiol*. **1**, 258-268. (DOI:10.1016/j.hrthm.2008.10.019)
 6. Das, M.K. & Zipes, D.P. 2009 Fragmented QRS: A predictor of mortality and sudden cardiac death. *Heart Rhythm*. **6**(3S), S8-S14, (march sup). (DOI:10.1016/j.hrthm.2008.10.019)
 7. Pietrasik, G., Goldenberg, I., Zdzienicka, J., Moss, A.J. & Zareba, W. 2007 Prognostic Significance of Fragmented QRS Complex for Predicting the Risk of Recurrent Cardiac Events in Patients With Q-Wave Myocardial Infarction. *Am J Cardiol*. **100**(4), 583-586. (DOI:10.1016/j.amjcard.2007.03.063)
 8. Guo, R., Li, Y., Tang, K. & Li, W. 2012 Significance of fragmented QRS complexes for identifying culprit lesions in patients with non-ST-elevation myocardial infarction: a single-center, retrospective analysis of 183 cases. *BMC Cardiovasc Disord*. **12**(44). (DOI: 10.1186/1471-2261-12-44)
 9. Homsy, M., Alsayed, L., Safadi, B., Mahenthiran, J., & Das, M.K. 2009 Fragmented QRS Complexes on 12-Lead ECG: A Marker of Cardiac Sarcoidosis as Detected by Gadolinium Cardiac Magnetic Resonance Imaging. *Ann Noninvasive Electrocardiol*. **14**(4), 319–326. (DOI:10.1111/j.1542-474X.2009.00320.x)
 10. Morita, H., Kusano, K.F., Miura, D., Nagase, S., Nakamura, K., Morita, S.T., Ohe, T., Zipes, D.P. & Wu, J. 2008 Fragmented QRS as a Marker of Conduction Abnormality and a Predictor of Prognosis of Brugada Syndrome. *Circulation*. **118**, 1697-1704. (DOI:10.1161/CIRCULATIONAHA.108.770917)
 11. Nagao, S., Watanabe, H., Kodama, M., Tanaka, J., Suzuki, E., Narita, I. & Aizawa, Y. 2011 Fragmented QRS Complexes, Conduction Disorder, and ST Segment Abnormality on Twelve-Lead Electrocardiography Predict Severe Cardiac Manifestation in Sarcoidosis. *Circulation*. **124**: A9485.
 12. Vanga, S.R., Koerber, S., DiBiase, L., Verma, A., Bommana, S., Swarup, V., Natale, A., Dawn, B. & Lakireddy, D. 2010 Prevalence of Fragmented QRS Complexes in Non-Ischemic Dilated Cardiomyopathy Patients and Long Term Prognosis. *Circulation*. **122**: A20836.
 13. Korhonen, P., Husa, T., Konttila, T., Tierala, I., Mäkitjärvi, M., Väänänen, H., Ojanen, J., Vehtari, A. & Toivonen, L. 2010 Fragmented QRS in Prediction of Cardiac Deaths and Heart Failure Hospitalizations after Myocardial Infarction. *annnoninvas electro*. **15**, 130-137. (DOI:10.1111/j.1542-474X.2010.00353.x)
 14. Refaat, M.M., Benhayon, D., Batal, O., Purohit, A., Halder, I., Mehd, H., Gutmann, R., Masry, H.E., Bloom, H.L., Dudley, S.C., Ellinor, P.T., Shalaby, A.A., Weiss, R., McNamar, D.M., Saba, S. & London, B. 2011 Fragmented Wide QRS on a 12-Lead Electrocardiogram Increases the Risk of Ventricular Arrhythmias in Patients with Severe Systolic Dysfunction. *Circulation*. **124**, A15244.
 15. Michael, M.A. & Das, M.K. 2006 Fragmented QRS on a 12-lead ECG is a Sign of Acute or Recent Myocardial Infarction. *Circulation*. **114**, II_512.
 16. Mazomenos, E.B., Chen, T., Acharyya, A., Bhattacharya, A., Rosengarten, J. & Maharatna, K. 2012 A Time-Domain Morphology and Gradient based Algorithm for ECG Feature Extraction. *Industrial Technology (ICIT), 2012 IEEE International Conference on*. **19**, 117-122, 19. (DOI:10.1109/ICIT.2012.6209924)
 17. Gao, G.Q. 2003 Computerised Detection and Classification of five Cardiac Conditions. Master thesis, AUT, Auckland, New Zealand.
 18. <http://www.chiron-project.eu/>
 19. Mazomenos, E.B., Biswas, D., Acharyya, A., Chen, T., Maharatna, K., Rosengarten, J., Morgan, J. & Curzen, N. 2013 A Low-complexity ECG Feature Extraction Algorithm for Mobile Healthcare Applications. *Information Technology in Biomedicine, IEEE Transactions on*. **17**(2), 459-469 (DOI: 10.1109/TITB.2012.2231312)
 20. Goernig, M., DiPietro Paolo, D., Haeuelsen, J. & Ern , S.E. 2008 Biomagnetic risk stratification by QRS fragmentation in patients with Implanted Cardioverter Defibrillators. *ECIFMBE 2008, IFMBE Proceedings*. **22**, 5–7. (DOI:10.1007/978-3-540-89208-3_2)
 21. Chatterjee, S. & Changawala, N. 2010 Fragmented QRS Complex: A Novel Marker of Cardiovascular Disease. *Clin. Cardiol*. **33**(2), 68–71. (DOI:10.1002/clc.20709)
 22. Pan, J. & Tompkins, W.J. 1985 A Real-Time QRS Detection Algorithm. *Biomedical Engineering, IEEE Transactions on*, **32**(3), 230-236. (DOI:10.1109/TBME.1985.325532)
 23. Sahambi, J.S., Tandon, S.N. & Bhatt, R.K.P. 1997 Using Wavelet Transforms for ECG Characterization: An On-line Digital Signal Processing System. *Engineering in Medicine and Biology Magazine, IEEE*. **16**, 77-83. (DOI:10.1109/51.566158)
 24. Mart nez, J.P., Almeida, R., Olmos, S., Rocha, A.P. & Laguna, P. 2004 A Wavelet-Based ECG Delineator: Evaluation on Standard Databases. *Biomedical Engineering, IEEE Transactions on*. **51**(4), 570-581. (DOI:10.1109/TBME.2003.821031)
 25. Rinc n, F., Recas, J., Khaled, N. & Atienza, D. 2011 Development and Evaluation of Multilead Wavelet-Based ECG Delineation Algorithms for Embedded Wireless Sensor Nodes. *Information Technology in Biomedicine, IEEE Transactions on*. **15**(6), 854-863. (DOI:10.1109/TITB.2011.2163943)
 26. Fugal, D. L. 2009 Conceptual Wavelets in Digital Signal Processing. *Space and Signals Technical Publishing*, San Diego, CA.
 27. Zhang, D. 2005 Wavelet Approach for ECG Baseline Wander Correction and Noise Reduction. *Engineering in Medicine and Biology Society, 2005. IEEE-EMBS 2005. 27th Annual International Conference of the*. **27**, 1212-1215. (DOI: 10.1109/IEMBS.2005.1616642)

* Author for correspondence (amit_acharyya@iith.ac.in)

28. Hostalkov'a, E.&Prochazka, A. 1905 Wavelet Signal And Image Denoising. Institute of Chemical Technology, Prague Department of Computing and Control Engineering Technick'a 166 28 Prague 6.
29. Li, S.& Lin, J. 2009 The Optimal De-noising Algorithm for ECG Using Stationary Wavelet Transform. *Computer Science and Information Engineering, 2009 WRI World Congress on.*6,469-473. (DOI: 10.1109/CSIE.2009.999)
30. Hernandez, O.&Olvera, E. 2009 Noise Cancellation on ECG and Heart Rate Signals Using the Undecimated Wavelet Transform*Health, Telemedicine, and Social Medicine, 2009. eTELEMED '09. International Conference on.* 145-150 (DOI:10.1109/eTELEMED.2009.49)
31. Baraniuk, R., Choi, H., Neelamani, R., Ribeiro, V., Romberg, J., Guo, H., Fernandes, F., Hendricks, B., Gopinath, R., Lang, M., Odegard, J.E.& Wei, D. Rice wavelet Toolbox. <http://www.dsp.rice.edu/software/rwt.shtml> , 2002.
32. Antoniadis, A., Bigot, J. & Sapatinas, T. 2001 Wavelet estimators in nonparametric regression: a comparative simulation study. *J Stat Software* **6**(6), 1 –83.
33. Goldberger, A.L., Amaral, L.A.N., Glass, L., Hausdorff, J.M., Ivanov, P.Ch., Mark, R.G., Mietus, J.E., Moody, G.B., Peng, C.K.&Stanley, H.E. PhysioBank, PhysioToolkit, and PhysioNet: Components of a New Research Resource for Complex Physiologic Signals. *Circulation*.**101**(23), e215-e220, 2000 (June 13).
34. Bousseljot, R., Kreiseler, D.& Schnabel, A. 1995 Nutzung der EKG Signaldatenbank CARDIODAT der PTB ber das Internet,," Biomedizinische Technik, Band 40, Ergnzungsband 1 S 317.
35. Loring, Z., Chelliah, S., Selvester, R.H., Wagner, G.& Strauss, D.G. 2011 A detailed guide for quantification of myocardial scar with the Selvester QRS score in the presence of electrocardiogram confounders. *J Electrocardiol*.**44**, 544–554. (DOI:10.1016/j.jelectrocard.2011.06.008)